

Rethinking convective quasi-equilibrium: observational constraints for stochastic convective schemes in climate models

BY J. DAVID NEELIN^{1,2,*}, OLE PETERS^{1,2}, JOHNNY W.-B. LIN³,
KATRINA HALES^{1,2} AND CHRISTOPHER E. HOLLOWAY^{1,2}

¹*Department of Atmospheric and Oceanic Sciences, and*

²*Institute of Geophysics and Planetary Physics, University of California,
Los Angeles, 405 Hilgard Avenue, Los Angeles, CA 90095-1565, USA*

³*Physics Department, Box 30, North Park University, 3225 West Foster
Avenue, Chicago, IL 60625, USA*

Convective quasi-equilibrium (QE) has for several decades stood as a key postulate for parametrization of the impacts of moist convection at small scales upon the large-scale flow. Departures from QE have motivated stochastic convective parametrization, which in its early stages may be viewed as a sensitivity study. Introducing plausible stochastic terms to modify the existing convective parametrizations can have substantial impact, but, as for so many aspects of convective parametrization, the results are sensitive to details of the assumed processes. We present observational results aimed at helping to constrain convection schemes, with implications for each of conventional, stochastic or ‘superparametrization’ schemes. The original vision of QE due to Arakawa fares well as a leading approximation, but with a number of updates. Some, like the imperfect connection between the boundary layer and the free troposphere, and the importance of free-tropospheric moisture to buoyancy, are quantitatively important but lie within the framework of ensemble-average convection slaved to the large scale. Observations of critical phenomena associated with a continuous phase transition for precipitation as a function of water vapour and temperature suggest a more substantial revision. While the system’s attraction to the critical point is predicted by QE, several fundamental properties of the transition, including high precipitation variance in the critical region, need to be added to the theory. Long-range correlations imply that this variance does not reduce quickly under spatial averaging; scaling associated with this spatial averaging has potential implications for superparametrization. Long tails of the distribution of water vapour create relatively frequent excursions above criticality with associated strong precipitation events.

Keywords: atmospheric moist convection; precipitation; stochastic parametrization; climate models

* Author and address for correspondence: Department of Atmospheric and Oceanic Sciences, University of California, Los Angeles, 405 Hilgard Avenue, Los Angeles, CA 90095-1565, USA (neelin@atmos.ucla.edu).

One contribution of 12 to a Theme Issue ‘Stochastic physics and climate modelling’.

1. Introduction

(a) *Overview*

Moist convection is among the most important of the physical processes occurring at small scales not resolved at the grid size of climate models, currently on the order of 100 km in the horizontal. The bulk effects of these small scales must be parametrized as a function of the large-scale variables. Convective quasi-equilibrium (QE) postulates that fast removal of buoyancy by moist convective up/downdraughts at small scales establishes a response of the ensemble mean convective heating, moisture sink and other properties that maintain statistical stationarity, balancing the large-scale flow, which is assumed to be slowly varying. Many variants of the associated closures lie at the heart of the parametrizations of moist convection in most current climate models, and similar considerations are relevant to numerical weather prediction models, despite their higher resolution.

Traditional parametrizations represent only the ensemble mean of the small scales as a deterministic function of a large-scale flow, disregarding fluctuations arising at the small scales. A sense that small-scale fluctuations are important motivated the development of stochastic convective parametrizations. The first generation of stochastic convective parametrizations may be viewed as a sensitivity study indicating that the impacts can indeed be substantial. However, stochastic parametrization introduces new parameters and processes; the climate solution exhibits some of the same dismaying sensitivity to these as it does to the traditional convective parametrization. Thus it becomes pressing to better characterize the statistics of convection in a manner that can inform stochastic convective parametrization and our understanding of convection in general. Observational work with this aim is the main theme of this paper.

After reviewing issues in QE stochastic convective parametrization in §2, we present observational results from current projects in §§3 and 4. We argue that these affirm some aspects of QE, but that some of these results suggest a new interpretation of QE that may be highly compatible with stochastic convective parametrization. We then discuss ways in which one might in the future bring these properties into representations of deep convection, discussing implications for both stochastic convection schemes and ‘superparametrization’ approaches.

(b) *Convective QE and motivation for stochastic schemes*

The original vision of convective QE is articulated in Arakawa & Schubert (1974): ‘When the time scale of the large-scale forcing, is sufficiently larger than the [convective] adjustment time, ... the cumulus ensemble follows a sequence of quasi-equilibria with the current large-scale forcing. We call this ... the quasi-equilibrium assumption.’ ‘The adjustment ... will be towards an equilibrium state ... characterized by ... balance of the cloud and large-scale terms ...’ Convection acts to reduce a measure of buoyancy, which in their parametrization is the cloud work function A (for each of a spectrum of entraining plumes).

The system is slowly driven by large-scale forcing (moisture convergence, evaporation and radiative cooling) generating conditional instability, while small-scale convection provides a fast dissipation of buoyancy. Above the onset threshold, strong convection and precipitation greatly increase, pushing the system quickly back towards onset values. Thus, a statistical equilibrium tends

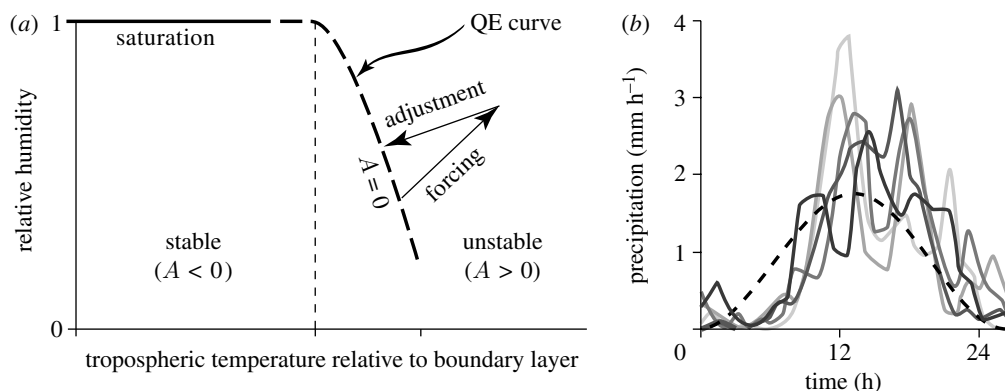


Figure 1. (a) Schematic of convective QE as envisioned by Arakawa & Schubert (1974). Adapted from Arakawa (2004). The line denoted ‘QE curve’ represents the statistical equilibrium towards which the system is postulated to be adjusted by deep convection, which is posited to act quickly relative to the large-scale forcing. The thick dashed part of this curve indicates zero buoyancy and the onset of convection through conditional instability (the solid line at relative humidity=1 corresponds to large-scale saturation). (b) Precipitation rates (solid curves) averaged over the 512 km domain from a two-dimensional cloud-resolving model (CRM) in response to an imposed large-scale forcing with cooling and moistening (dashed curve). A sequence of five different time intervals responding to repetitions of the same forcing are overlaid. The large variations from one instance to another, even for these domain averages, are departures from QE. Adapted from Xu *et al.* (1992).

to be established among buoyancy-related fields: temperature T and moisture q , including their vertical structures, are constrained. Arakawa (2004) provided a schematic, shown here in figure 1a, for the original QE postulate.

There are, however, several issues regarding QE that need to be addressed. First, using a finite adjustment time scale makes a difference in the behaviour, as does the value of the adjustment rate or plume closures affecting this (Betts & Miller 1986; Gregory & Rowntree 1990; Emanuel 1991, 1993; Moorthi & Suarez 1992; Emanuel *et al.* 1994; Yu & Neelin 1994; Zhang & McFarlane 1995; Pan & Randall 1998). Furthermore, the ensemble size of deep convective elements in a typical climate model (order of 100 km) grid box over a 10–30 min time increment is not large. One should expect variance about the ensemble mean in such an average. This variance can drive large-scale variability (even more so in the presence of mesoscale organization). Another issue relates to complex influences on vertical structures, such as convectively coupled wave modes (Straub & Kiladis 2003; Haertel & Kiladis 2004; Tian *et al.* 2006) discussed in §3. Raymond (1997) noted a tendency for the atmospheric boundary layer (ABL) to reach its own form of QE, mostly between surface fluxes and convective downdraughts, even as the free troposphere is being affected by remote wave dynamics.

Figure 1b shows an example from Xu *et al.* (1992) that motivated our own interest in stochastic convection schemes. Different instances of precipitation are shown from a cloud-resolving model (CRM) averaged over a domain that might roughly compare with a large-scale model grid (albeit from a two-dimensional CRM) for a case with shear, promoting mesoscale organization. The following three features may be noted: (i) Xu *et al.* (1992) concluded that the similarity among realizations was sufficient for convection to be parametrizable, (ii) there is a substantial lag of the onset of rainfall relative to the large-scale forcing,

suggesting that convective processes are not as quickly adjusting as originally hoped, and (iii) there is much variance among realizations for the same large-scale forcing—capturing these departures from QE is the motivation for stochastic parametrizations discussed in §2.

Superparametrization (e.g. Grabowski 2001; Khairoutdinov & Randall 2001; Randall *et al.* 2003), in which a few small grid cells of a CRM are embedded within each large-scale grid point, retains (and potentially exaggerates) fluctuations associated with small scales. It also aims to address a host of issues such as the accurate representation of convective plumes and the level of detrainment for cloud water. We thus also discuss the implications of observations of precipitation variance for superparametrization.

(c) *Simple considerations in the moisture and thermodynamic equations*

For reference, the temperature and moisture equations are provided here, along with considerations used in subsequent sections,

$$\partial_t T + \nabla \cdot s\mathbf{v} + \partial_p(s\omega) - K_T \nabla^2 s + C_K = Q_c + \partial_p(F_R + F_T), \quad (1.1)$$

$$\partial_t q + \nabla \cdot q\mathbf{v} + \partial_p(q\omega) - K_q \nabla^2 q = -Q_q + \partial_p F_q, \quad (1.2)$$

where dry static energy $s = T + \phi$ and ϕ is geopotential, with heat capacity at constant pressure c_p absorbed into temperature T , latent heat of condensation absorbed into specific humidity q and acceleration due to gravity absorbed into pressure p ; \mathbf{v} is horizontal wind; Q_c is convective heating; $-Q_q$ is the moisture sink; F_R , F_T and F_q are vertical (diffusive for T and q) fluxes of radiation, sensible heat and moisture, respectively; and ω is vertical velocity in pressure coordinates. K_T and K_q are horizontal diffusivities parametrizing small-scale mixing. C_K is conversion to kinetic energy (sometimes neglected in (1.1)).

To provide a thumbnail sketch of how a QE scheme can be implemented, consider that one has some model of a convective plume that yields a temperature T_c of the convective element as a function of pressure, and of the large-scale T and q . In the simplest case of a plume rising adiabatically from the boundary layer, T_c is just the moist adiabat; inclusion of entrainment produces a dependence on environmental T and q in the free troposphere. The buoyancy depends on the difference $T_c - T$ (actually the virtual temperature, including direct effects of specific humidity on density, but for presentation purposes we omit the details of this). One such measure is convective available potential energy (CAPE), which can be written as $A = R_d \int (T_c - T) d \ln p$, where R_d is the gas constant of dry air (Emanuel 1994). Arakawa & Schubert (1974) and related schemes used a cloud work function for a spectrum of entraining plumes with differing T_c .

QE closures typically postulate that a weighted vertical integral measure of buoyancy is rapidly reduced. The simplest case is typified by the Betts & Miller (1986, BM) convective adjustment scheme, in which

$$Q_c = (T_c - T + \xi)/\tau_c, \quad Q_q = (q_c(T) - q + \xi)/\tau_c, \quad (1.3)$$

whenever the vertical integrals of these quantities are positive. This scheme tends to reduce $(T_c - T)$ level by level when moisture exceeds a critical value $q_c(T)$. In (1.3), BM is shown with a stochastic term, ξ , to be described later ($\xi = 0$ for the standard BM scheme).

Parallels can be seen in the Zhang & McFarlane (1995, ZM) convective scheme in which the closure assumption $M_b F \equiv A/\tau_c$ creates a tendency for CAPE, A , to be reduced exponentially

$$\partial_t A + \dots = -M_b F \equiv (A + \xi)/\tau_c, \quad (1.4)$$

where τ_c is an assumed convective time scale (=2 hours); M_b is the updraught cloud base mass flux; and F is the rate of CAPE removal per unit M_b from a cloud plume model. A stochastic component ξ will be defined later; $\xi=0$ for the standard ZM scheme.

The energy constraint that the vertical mass-weighted integral $\hat{\cdot}$ of convective heating equals latent heat by moisture loss implies

$$\hat{Q}_c = \hat{Q}_q. \quad (1.5)$$

If most of the condensed water falls out of the system within the grid box, then the precipitation will be approximately given by $P = \hat{Q}_q$.

Several points may be noted regarding (1.5). First, in any stochastic term the convective heating should be matched by a corresponding moisture sink, respecting (1.5), or it will produce unphysical effects. Second, (1.5) can have substantial effects within convection schemes; in (1.3), for instance, it implies that T_c is determined by $[\hat{q}_c - \hat{q} + \hat{T}]$ (Neelin & Zeng 2000). Third, (1.5) implies that summing vertical integrals of (1.1) and (1.2) yields an equation (the moist static energy budget) in which the convective heating does not appear. Thus variations in the heating do not directly change the sum $(\hat{T} + \hat{q})$. The column water vapour, $w = \hat{q}$, also known as precipitable water, will be important in observational analysis below, where we use the symbol w for consistency with other work.

If QE ties moisture and temperature closely together when convection is occurring, so that moisture is slaved to \hat{T} , an approximation used in some theoretical considerations (e.g. Emanuel *et al.* 1994), then the moist static energy equation governs the thermodynamics to a leading approximation. If so, stochastic variations in convective heating and precipitation would have little effect on the large-scale dynamics. This indicates the potential importance of departures from strict versions of QE. Variations in Q_c of sufficiently large amplitude relative to the mean will frequently shut down convection. This removes any QE constraints until the convection begins again. Smoothly posed QE schemes tend to operate rather more continuously than observed convection, so one principal effect of stochastic convection schemes is to intermittently break the QE constraints. We will argue below that the large ensemble average envisioned in the original posing of QE is a first approximation, rather than a constraint applying at short time scales. The intermittent departures from QE are inherent properties of convection, and it should be possible to set up the physics of stochastic schemes to include this in a manner that mimics convection.

2. Issues in stochastic deep convective parametrization

(a) Implementations of stochastic convective parametrization

Given the deterministic convection schemes operating under QE constraints, a scheme that randomly perturbs the system from QE would be a reasonable first approach to stochastic parametrization; this was indeed the method used in the

earliest attempts. [Buizza *et al.* \(1999\)](#), for instance, perturbed all parametrized quantities using a uniform distribution in order to test the effects of such a representation of model error on ensemble spread. [Yu & Neelin \(1994\)](#) noted that noise could support tropical wave variability in a simplified primitive equation model.

[Lin & Neelin \(2000\)](#), seeking to represent fluctuations in convection arising at the small scales, such as those seen in [figure 1b](#), introduced stochastic perturbations to large-scale CAPE in a BM convective parametrization in an intermediate-complexity atmospheric model. Noise ξ from a first-order autoregressive (Markov) process was added to the difference $T_c - T$ as in (1.3). In an alternate stochastic scheme, an empirically estimated precipitation distribution (lognormal, with separately parametrized probability of zero precipitation), adjusted at each time step to match the mean of the deterministic convective scheme, provided stochastic convective heating ([Lin & Neelin 2002](#)).

[Lin & Neelin \(2003\)](#) described two stochastic parametrizations implemented in the National Center for Atmospheric Research Community Climate Model (CCM3): the CAPE- M_b and vertical structure of heating (VSH) schemes. In the CAPE- M_b scheme, random variations are introduced to the relationship between cloud base mass flux (M_b) and CAPE. Physically, the random component may be thought of as grid-scale response to subgrid variability. Thus, a noise perturbation ξ is added to CAPE, as in (1.4). The VSH scheme is a first-cut look at effects of stochastic vertical structure variations, for instance, corresponding to variation in detrainment levels of convective elements. Noise ξ is introduced as a perturbation to temperature at each level, with $\xi = 0$ to ensure moist static energy conservation and to contrast with the CAPE- M_b scheme where ensemble mean heating is directly perturbed.

[Majda & Khouider \(2002\)](#) defined a stochastic model based on small-scale convective inhibition (CIN) and coupled this model with a prototypical mass-flux convective parametrization through area fraction for deep convection, boundary-layer equivalent potential temperature and stratiform mass flux. Inclusion of the scheme produces eastward propagating convectively coupled waves that qualitatively resemble observations ([Khouider *et al.* 2003](#)).

[Berner *et al.* \(2005\)](#), following the suggestion of [Palmer \(2001\)](#), implemented an additional stochastic forcing on streamfunction based on a cellular automata model aiming to represent the mesoscale organization of convective systems in the European Centre for Medium-Range Weather Forecasts (ECMWF) Integrated Forecasting System (IFS). Madden–Julian oscillation (MJO)-like variability results, though without a spectral peak. [Tompkins & Berner \(in press\)](#) implemented a scheme in the ECMWF IFS, applying a uniformly distributed stochastic input to humidity, which then influences triggering and updraught humidity in the deterministic convective parametrization. This scheme results in increased ensemble spread, though less so than the [Buizza *et al.* \(1999\)](#) scheme. Combining the two schemes increases prediction skill in mid-latitudes, though with mixed results in the tropics.

[Teixeira & Reynolds \(2008\)](#) applied a stochastic component to select tendencies related to the convective parametrization in the Navy Operational Global Atmospheric Prediction System weather prediction model. The stochastic component is drawn from a normal distribution and is applied to the tendency calculated by the deterministic parametrization. This results in significant

ensemble spread in dynamical variables such as 500 hPa geopotential height and winds. Plant & Craig (2008) drew random values in cloud base mass-flux-related variables from distributions motivated by statistical mechanics considerations (Craig & Cohen 2006), and calculated convective tendencies using the deterministic Kain & Fritsch (1990) cloud model. Tests of the scheme in a single-column model yield results consistent with mean temperature and humidity profiles from CRM simulations.

Stochastic convective schemes so far have focused on the thermodynamic aspects of convection; it is worth noting parallel efforts to parametrize mesoscale circulations and momentum transport (e.g. Moncrieff & Klinker 1997; Moncrieff & Liu 2006) or to give subgrid-scale plumes more individual identity (Kuell *et al.* 2007), directions that may be highly useful to future stochastic parametrization.

(b) Sensitivity to stochastic parametrization

Just as simulated climate and variability are sensitive to different deterministic convective schemes (Maloney & Hartmann 2001; Tost *et al.* 2006), one can expect corresponding sensitivity to the introduction of the stochastic parametrization schemes described in §2*a*. Even the early simple tests of stochastic parametrization produced substantial effects. Buizza *et al.* (1999) found improved forecast skill as a result of the inclusion of a stochastic representation for model error. Lin & Neelin (2000) found in their perturbations to model CAPE that, depending on the autocorrelation time, the stochastic scheme improved the simulated probability distribution of daily mean precipitation in tropical regions. For grid-scale noise at a 1-day *e*-folding time scale, the scheme enhanced intraseasonal equatorial wavenumber-one 850 hPa zonal wind spectra power.

With substantial impacts comes substantial sensitivity, and new parameters requiring observational constraints. For instance, Lin & Neelin (2000) found their stochastic CAPE scheme to be sensitive to the autocorrelation time scale of the input noise, suggesting that time-scale parameters associated with prognostic convective or mesoscale elements will need to be quantified in future schemes. Tests with Lin & Neelin's (2002) empirical stochastic parametrization showed such strong interaction of the heating with large-scale dynamics that they concluded that a stochastic parametrization cannot be calibrated off-line. Rather, comparison to observations should be done with output from a full model simulation.

The importance of this model feedback can be seen in the intraseasonal response to stochastic convective schemes. If a deterministic climate model's interaction of convection with large-scale dynamics yields damped MJO-like intraseasonal variability, a stochastic scheme will act to enhance that MJO-like variability to more closely resemble observations, as in the Lin & Neelin (2000) example. In contrast, if a deterministic climate model does not have a clear mode that yields MJO-like variability, the impact of a stochastic scheme will be less straightforward. As a detailed example, we consider the effects of the stochastic convective parametrizations of Lin & Neelin (2003), joined to the ZM convective parametrization (as described in §1*c*).

Figure 2 shows equatorial precipitation and 850 hPa zonal wind, u_{850} , spectral power for the CAPE- M_b and VSH schemes of Lin & Neelin (2003), compared to a CCM3 control run. The format follows figs 4 and 5 of Maloney & Hartmann (2001), which provides observations and deterministic convection scheme results.

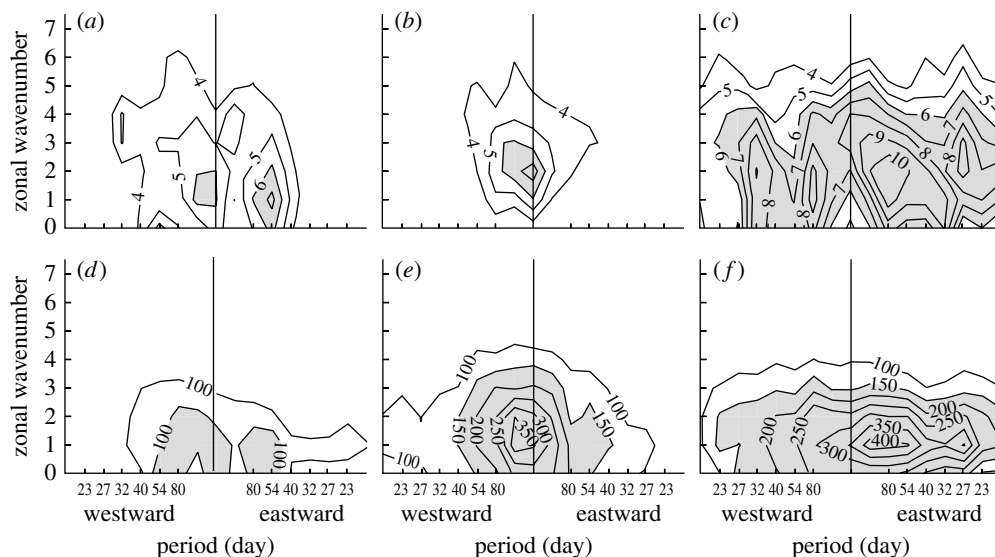


Figure 2. Zonal wavenumber versus period plot of equatorial spectra of (a) control run precipitation, P , (b) CAPE- M_b scheme precipitation, (c) VSH scheme precipitation, (d) control run 850 hPa zonal wind, u_{850} , (e) CAPE- M_b scheme u_{850} , and (f) VSH scheme u_{850} . The spectra are shaded above 6 units of 10^4 (W m^{-2})² for precipitation and above 150 (m s^{-1})² for u_{850} . The spectral estimator has a standard deviation of 10%. See Lin & Neelin (2003) for analysis details.

While the inclusion of stochastic variance can increase spectral power, it does not necessarily excite the portion of the wave spectrum corresponding to observed intraseasonal variability. For instance, in the CAPE- M_b scheme, spectral power in both u_{850} and precipitation is shifted to lower frequency westward waves. Spectral power in u_{850} increases notably, but precipitation power remains nearly unchanged. The VSH scheme dramatically increases spectral power in u_{850} and precipitation, but it excites a broad range of wave frequencies, both eastward and westward propagating. Such results suggest that tuning stochastic convective parametrizations may be as difficult as tuning the deterministic parametrizations they are meant to improve.

Efforts have been made to constrain the formulation of stochastic parametrizations using arguments from first principles and statistics from CRMs. For instance, using principles from equilibrium statistical mechanics, for the case of negligible plume–plume interaction, Craig & Cohen (2006) derived an analytical expression for the probability distribution of total cloud mass flux over a region. Cohen & Craig (2006) confirmed these theoretical results using CRM simulations. CRM modelling by Shutts & Palmer (2007) also confirmed the findings of Craig & Cohen (2006) that individual cloud mass flux follows a Boltzmann exponential distribution, though Shutts & Palmer (2007) found a different dependence between the mean and standard deviation of coarse-grained effective temperature tendencies than that was predicted by Craig & Cohen (2006).

While CRM studies are valuable, there is a clear need to derive additional constraints on the stochastic parametrization problem from observations. In the next section, we discuss results aimed at better characterizing the statistics of observed convection at short time scales and small space scales.

3. Vertical structure associated with QE

Several studies have indicated that tropical temperature profiles are constrained towards convective plume temperatures lifted from warm, moist ABL conditions, approximated by moist adiabats (Xu & Emanuel 1989; Brown & Bretherton 1997) or including entrainment (Kuang & Bretherton 2006), as predicted by QE. Figure 3*a,b* shows temperature perturbations from radiosondes at different pressure levels regressed on their free-tropospheric vertical averages along with correlations, as well as similar regressions made using an ensemble of reversible moist adiabats raised from typical tropical surface conditions. Both the monthly Comprehensive Aerological Reference Dataset (CARDS; Eskridge *et al.* 1995) averages and the daily Tropical Ocean Global Atmosphere Coupled Ocean–Atmosphere Response Experiment (TOGA–COARE) data (Ciesielski *et al.* 1997) show fairly good agreement with QE predictions (the moist adiabatic curve) in the free troposphere. The negative deviations aloft are due to dynamical constraints as discussed in Holloway & Neelin (2007). The departures from QE expectations in the ABL (consistent with Brown & Bretherton (1997)) may be interpreted in terms of wave dynamics spreading the temperature signal horizontally from localized convection in the free troposphere, while competing effects from surface fluxes occur in the ABL. The lower correlations indicating less vertical coherence at higher time resolution fits with several recent studies showing that there are more complicated vertical temperature perturbation structures at these scales associated with tropical wave features (e.g. Straub & Kiladis 2003; Haertel & Kiladis 2004).

Overall, observations of tropical temperature perturbations such as those in figure 3*a,b* show fairly good agreement, especially at larger scales and in the free troposphere, with the idea of a dominant vertical structure that is not far from moist adiabatic as hypothesized from QE constraints. Figure 3*c* (adapted from C. E. Holloway & J. D. Neelin 2008, unpublished manuscript) shows that moisture vertical structure, conditionally averaged on precipitation, also varies most in the free troposphere, whereas there are smaller changes in the ABL. These profiles are made using 5 years of radiosondes and optical gauge 60 min precipitation averages at the Nauru Island (0.5° S, 166.9° E) Atmospheric Radiation Measurement (ARM) Program observation site (Stokes & Schwartz 1994). Figure 3*c* supports growing evidence in the literature that traditional convective parametrizations, which tend to emphasize the ABL moist static energy, are not giving enough weight to the role that lower free-tropospheric dryness plays in suppressing deep convection (e.g. Parsons *et al.* 2000; Raymond 2000; Grabowski 2003; Derbyshire *et al.* 2004). While QE thinking has in principle always included entrainment (Arakawa & Schubert 1974), more emphasis must be placed on accurately taking free-tropospheric moisture into account. Recently there have been increasing efforts to include these processes in current schemes (e.g. Zhang & Mu 2005; Zhang & Wang 2006).

Analysis of the Nauru ARM sonde data suggests that most of the q variance associated with w variance occurs in the lower free troposphere above the ABL, although there is also a small but significant q variance in the ABL associated with w variance. Figure 4*a* shows precipitation and entraining CAPE conditionally averaged on w for the ARM data (C. E. Holloway & J. D. Neelin 2008, unpublished manuscript). The sharp pickup of precipitation at a high enough value of w agrees

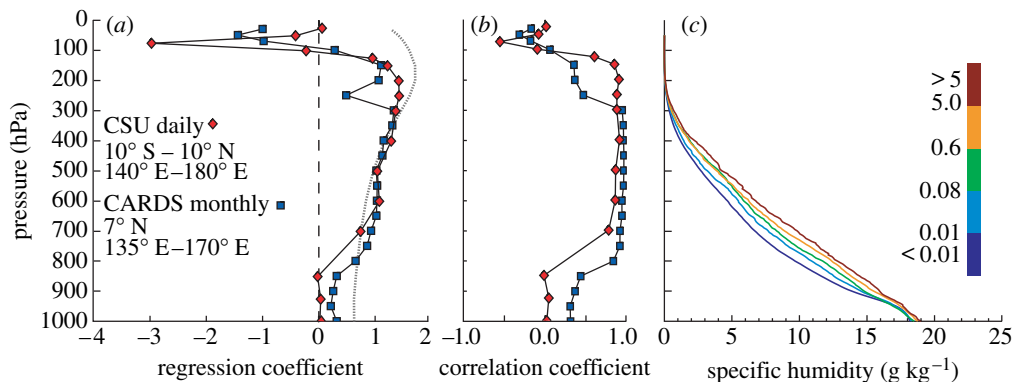


Figure 3. (a) Vertical temperature structures and (b) correlations, adapted from Holloway & Neelin (2007), associated with free-tropospheric average temperature perturbations, using CARDS monthly anomalies and Colorado State University (CSU) TOGA-COARE daily averages. The dashed grey line in (a) shows similar regressions for the moist adiabat (CARDS case shown; CSU case nearly identical below 300 hPa). (c) Nauru ARM q profiles from twice-daily radiosondes conditionally averaged on 60 min average optical gauge precipitation (bins give in colour bar in mm h^{-1}).

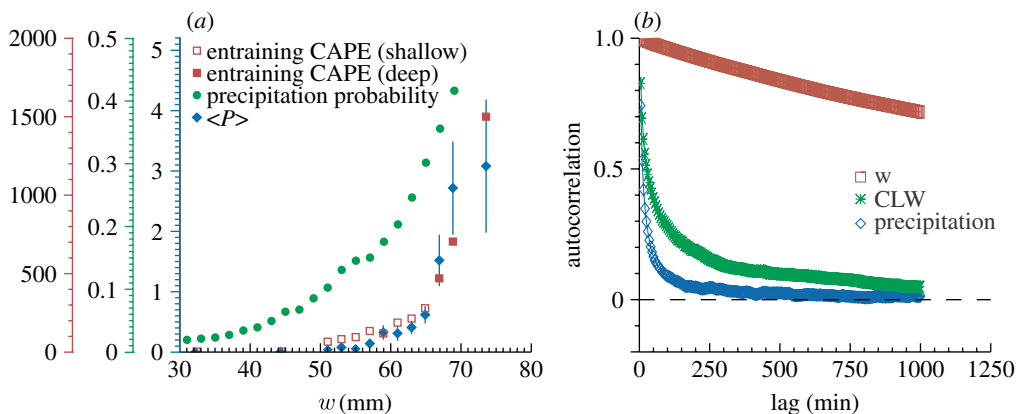


Figure 4. (a) Nauru ARM precipitation $\langle P \rangle$ (mm h^{-1} ; blue diamonds) as 60 min averages conditionally averaged on column water vapour w from radiosondes, with bars showing ± 1 standard error; entraining CAPE (J kg^{-1}) measured from lifting condensation level to level of neutral buoyancy (LNB) for 1000 hPa lifted parcels subjected to constant mixing, for the same w bins, with deep convective cases (LNB levels above 450 hPa) marked as red filled squares (open squares otherwise); precipitation probability (green dots) in next hour, given 5 min average w and 0 rain at time 0, from ARM MWR and optical gauge data. Colours of y-axes correspond to those of the symbols. (b) Autocorrelations for 5 min average w , cloud water and precipitation from ARM MWR and optical gauge data. The w bin edge values for (a) (in mm) are: less than 35, 35–50, every 2 mm from 50 to 70, and greater than 70; for precipitation probability curve, 2 mm bins from 30 to 70.

with satellite analyses in Bretherton *et al.* (2004) and Peters & Neelin (2006). The entraining CAPE (Brown & Zhang 1997), taken for the positively buoyant part of the path of lifted 1000 hPa parcels entraining 0.1% of environmental air per hPa (so that the virtual T_c from §1c includes mixing with T), also shows a sharp pickup, which appears to be due to both the moister free troposphere and the slightly higher ABL moist static energy associated with larger w . The CIN is always below 6 J kg^{-1}

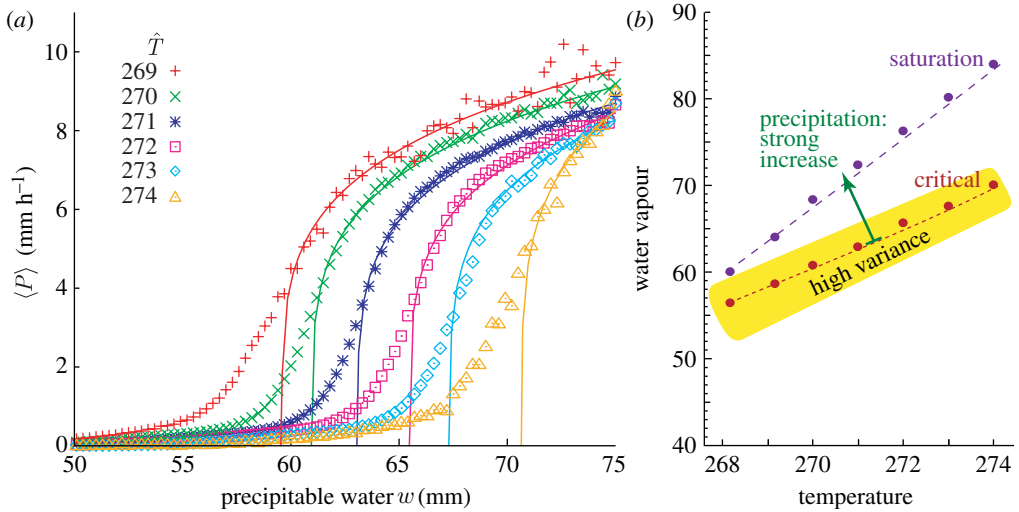


Figure 5. (a) Pickup of ensemble-average precipitation $\langle P \rangle$ in each 0.3 mm bin of column water vapour w for 1 K bins of the vertically averaged tropospheric temperature \hat{T} . Western Pacific $\langle P(w, \hat{T}) \rangle$ as a function of w for $\hat{T} = 269\text{--}274$ K; lines show power-law fits above criticality of the form (4.1). (b) The critical value of column water vapour w_c at which the onset of strong convection occurs, as a function of vertically averaged tropospheric temperature \hat{T} ; dots give the values determined as in (a), here combined from the tropical west Pacific, east Pacific and Atlantic. The vertically integrated saturation value of water vapour is also shown. Schematic elements indicate the pickup in precipitation and the band of high precipitation variance near criticality.

for these composite profiles, and there is no obvious relationship between CIN and the precipitation pickup. The three highest CAPE values have average levels of neutral buoyancy (which would theoretically correspond to cloud-top heights) approximately 150 hPa instead of below the 450 hPa level for the other bins (although these values are rather sensitive to choices of mixing profiles and adiabatic processes). Column water vapour w , which is readily available from satellites, therefore acts as more than a proxy for conditions conducive to deep convection; it is associated with both ABL and free-tropospheric contributions to buoyancy due to entrainment. As figure 4b illustrates, w also has significantly higher temporal autocorrelations than cloud water and precipitation (as seen in ARM microwave radiometer (MWR) and optical gauge data), suggesting that it can be thought of as a relatively slowly varying environmental control variable on which to compute statistics of sporadically occurring precipitation. Column water is also potentially useful for convective scheme transition probabilities (or trigger functions). The ARM MWR data in figure 4a show that probabilities of precipitation for the next hour, given no current precipitation, increase dramatically at high values of w .

4. Characteristics of the transition to strong convection

Examining the transition to strong convection at high time resolution, Peters & Neelin (2006) noted that the statistical properties of precipitating convection conform to those observed near continuous phase transitions, known as critical

phenomena. The observed properties include a rapid pickup of precipitation, P , above a critical value of precipitable water, w_c . The ensemble average, $\langle P \rangle$, conditioned on w , approaches a power law above criticality

$$\langle P \rangle(w) = a[(w - w_c)/w_c]^\beta, \quad \text{if } (w - w_c) > 0. \quad (4.1)$$

This is in contrast to a linear relation assumed in some convective parametrizations such as (1.3). Here this relationship is seen in [figure 5a](#) with column water vapour and precipitation retrievals ([Hilburn & Wentz 2007](#)) from the Tropical Rainfall Measuring Mission Microwave Imager (TMI), with the added dimension that it is examined for various values of vertical average tropospheric temperature \bar{T} from ERA40 reanalysis ([Uppala & coauthors 2005](#)).

Another confirmed expectation from the theory of phase transitions is a peak in the precipitation variance, σ_P^2 , near w_c ([figure 6a](#)). These properties are related to long-range spatial correlations in the critical region, observed as a non-trivial power-law dependence of the precipitation variance on the spatial averaging scale ([Peters & Neelin 2006](#)), implications of which will be discussed in §5c. Power-law dependence of fluctuations on averaging scale has been previously observed in the time domain for CAPE ([Yano *et al.* 2001](#)).

The amplitude a and the critical value w_c , in (4.1), are expected to be sensitive to the details of the processes involved. The exponent β , on the other hand, is predicted to be robust. This was confirmed observationally: β is comparatively invariant under changes of ocean basin ([Peters & Neelin 2006](#)) or temperature. While critical values, $w_c(T)$, and amplitudes $a(T)$ needed to be adjusted for each value of (vertically averaged) tropospheric temperature in [figure 5a](#), no changes were made to β . Rescaling the water vapour axis with $w_c(T)$ and the precipitation axis with $a(T)$, the curves collapse ([figure 6a](#)). The dependence of the critical value, w_c , on tropospheric temperature is shown in [figure 5b](#). Rather than w_c being a constant fraction of saturation, at higher temperature the transition occurs at greater subsaturation.

[Figure 6a](#) is a direct observational assessment of the QE postulate. It shows the distribution of observed water vapour values (the four upper curves), conditioned on non-zero precipitation rate. Most notably, the distribution is clearly peaked in the vicinity of the critical point, with the frequency of observed occurrences decreasing fast for increasing water vapour values. In other words, the system spends most of its precipitating time near the transition to convection, as predicted by QE.

The precipitation variance, shown in [figure 6a](#) (the four middle curves), is an indicator of the susceptibility of the system. A high intrinsic variance (and therefore susceptibility) near the QE state is expected if the QE state can be identified with the critical point of a continuous phase transition. The observed variance peaks near the critical point identified from the order parameter pickup (ensemble-average precipitation pickup, also shown in [figure 6a](#)). In principle, this could be the result of unresolved variations in water vapour or other variables, coupled with the fact that precipitation changes most rapidly here. The theory of critical phenomena, however, suggests high variance to be an intrinsic property of the system which is not due to insufficient measurement resolution. [Figure 6b](#) shows the event-size distribution for the Nauru ARM site

optical gauge precipitation. The event size is the rain integrated over an event, defined as consecutive measurements of non-zero rain rate (Peters *et al.* 2002). Event size is proportional to the energy released and has clear analogues in other self-organized critical systems. The scale-free distribution of event sizes is further evidence of the extreme sensitivity of the system.

5. Prototypes for these observed properties and implications

We use this section to further discuss some of the observed properties in the light of what is known from simpler prototype models.

(a) *A simple model exhibiting critical phenomena*

System-wide self-organization towards critical points of continuous phase transitions is a well-established field of research in statistical mechanics. In self-organized critical systems, of which moist convection appears to be an example, energy-dissipation rates (order parameters such as precipitation) pick up as a function of energy density (tuning parameters such as column water vapour). Perhaps the simplest model displaying such behaviour was introduced by Manna (1991). It is defined on a lattice to which particles are added. A hard-core repulsion is implemented, such that each site can harbour not more than one particle. Wherever this local threshold is surpassed, particles topple to randomly chosen neighbouring sites, where they can induce further topplings, leading to system-wide avalanches that transport particles to the open boundaries where they are dissipated.

The overall effect of these dynamics is an attraction to the critical point of an underlying absorbing-state phase transition (Tang & Bak 1988; Dickman *et al.* 1998). These dynamics are best demonstrated using a small system where finite-size effects are similarly important as they seem to be in the atmosphere. Figure 7 shows data for a system of 20×20 sites. Although the model is clearly not a representation of moist convection, it exhibits properties that can be qualitatively compared with those observed for convection in figure 6.

A high energy density in the system leads to activity, defined as the density of unstable sites during avalanches (blue pluses in figure 7a). Activity in turn reduces the energy density through dissipation at the open boundaries. Since a new particle is added whenever the system has avalanched into a stable configuration, it hovers around criticality (turquoise symbols in figure 7a). In the case of the Manna model, the self-organization towards criticality is so strong that we need to force the system away from criticality to explore the underlying phase transition. This is done here by implementing periodic boundaries such that no self-organization takes place and we can fully control the particle density (which is now conserved). The critical point is characterized by a divergence of the system's susceptibility to perturbations. This is reflected in the peak in the order parameter variance (pink crosses in figure 7a).

This extreme sensitivity is also expressed by the distribution of avalanche sizes. Here we count the number of local topplings, starting from the addition of a particle and ending at a new stable configuration. The probability distribution of such energy-release events is scale free and reminiscent of event-size distributions

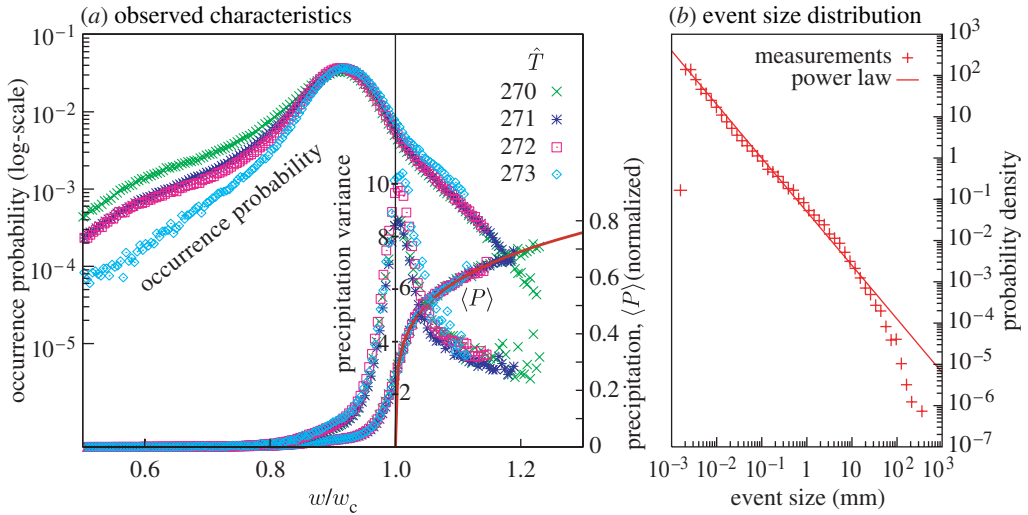


Figure 6. (a) Western Pacific observed characteristics from TMI data as a function of column water vapour normalized by the critical value w_c for each value of \hat{T} : probability density function of w for precipitating points (four upper curves), precipitation variance conditioned on w (four middle curves) and precipitation pickup curve (non-dimensionalized by amplitude a from (4.1) for each \hat{T}). (b) The precipitation event-size distribution for the Nauru ARM site time series.

observed at Nauru, figure 6b, as well as those in the mid-latitudes (Peters *et al.* 2002). In figure 7b we show the avalanche-size distribution along with its known exponent; in the thermodynamic limit of infinite system size, the distribution would follow a power law over an infinite range. The analogy with atmospheric event-size distributions suggests they can occur even for fixed, slow forcing—in other words, a scale-free range of precipitation events is associated with the organization towards the critical point in QE.

(b) *Implications of the exponential tails*

In figure 6a it was shown that the distribution of the atmospheric tuning parameter (the water vapour) has strongly non-Gaussian tails. There is a Gaussian-like core, but the tails are much better described by exponentials. One effect of these exponential tails is that we are able to observe the underlying phase transition. In the Manna model, the distribution is highly Gaussian, with the result that occurrences drop very rapidly above the critical point in the self organizing case. To observe the behaviour above criticality, we needed to introduce periodic boundaries. The question remains how it is possible that the atmosphere ever fluctuates as far from criticality, or QE, as it does.

A possible answer is provided by tracer dispersion in forced advection–diffusion problems, in which the tracer probability density distribution can have a Gaussian core with exponential tails (e.g. Gollub *et al.* 1991; Majda 1993; Shraiman & Siggia 1994). This can occur, for instance, in the two-dimensional case

$$\partial_t q + \mathbf{v} \cdot \nabla q - \kappa_0 \nabla^2 q = f, \tag{5.1}$$

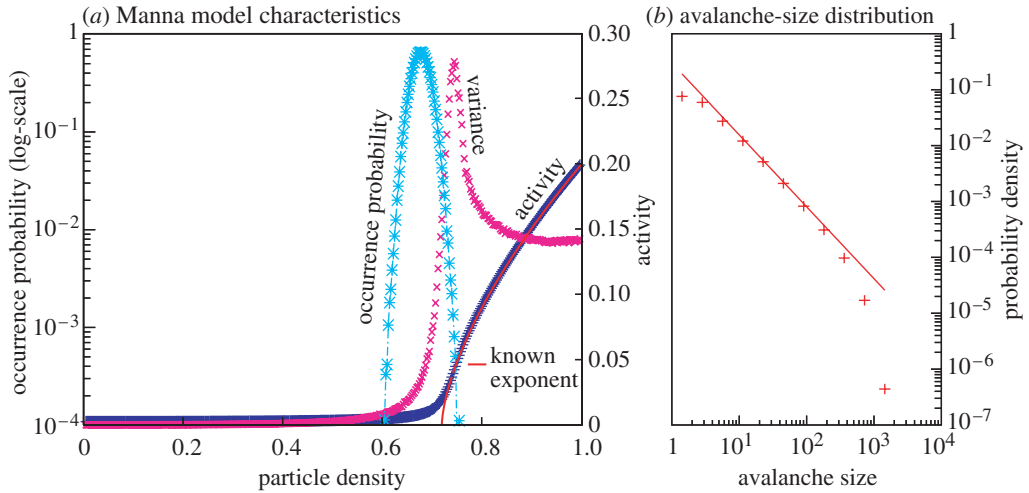


Figure 7. The characteristics of a two-dimensional Manna model of size 20×20 . (a) As a function of the tuning parameter (the density of particles in the system) the order parameter pickup (blue pluses) is shown along with its known exponent (red line; Lübeck 2000), for the case of a closed system. This is similar to $\langle P \rangle$ in figure 6a. The probability for the system to be found at a given particle density under conditions of self-organization (turquoise symbols, logarithmic scale) is Gaussian, like the core of the distribution in figure 6a. Also shown is the order parameter variance (closed system, pink crosses, arbitrary units), which looks much like that in figure 6a. (b) Avalanche-size distribution. The straight line indicates the exponent known from numerical work, e.g. by Lübeck (2000). Pluses, measured distribution.

with \mathbf{v} a non-divergent random flow field, when a large-scale gradient of tracer q is maintained (Shraiman & Siggia 1994) or when including a forcing f , such as Gaussian random forcing or resetting q in strips (Pierrehumbert 2000).

There are parallels to this in the vertical integral of the moisture equation (1.2),

$$\partial_t \hat{q} + \widehat{\mathbf{v} \cdot \nabla q} + \widehat{q \nabla \cdot \mathbf{v}} - K_q \nabla^2 \hat{q} = -P + E, \tag{5.2}$$

where P and E denote loss and gain terms due to precipitation and evaporation. Lower tropospheric advection is important (Parsons *et al.* 2000), with water vapour acting at first order like a passive tracer until convection begins. Evaporation and moisture divergence terms tend to set a large-scale gradient. The question of whether the complex loss term by precipitation and its feedbacks with moisture convergence act sufficiently like f in (5.1) to explain the exponential tails can presumably be answered by analysing models of various degrees of complexity between (5.1) and full CRM.

(c) Variance about QE and the superparametrization variance estimation problem

Superparametrization approaches (Randall *et al.* 2003) aim to estimate the statistics for a large-scale model grid cell from an embedded CRM. Computation time constraints imply that smaller grid cells of this model can cover only a small fraction of the area of the large-scale model cell—otherwise one would incur the computational cost of running the CRM globally. The variance scaling in the critical region has potential implications for this.

The following back-of-the-envelope argument suggests the likelihood that if the CRM were to produce the correct variance at the scale of its own grid cells, then the superparametrization approach would tend to overestimate the variance appropriate to the larger grid size. Consider coarse graining onto a larger $L \times L$ grid the results, say precipitation, of a CRM run at high resolution over a large domain. The averaging process reduces the variance. If the precipitation were spatially uncorrelated (from one high-resolution cell to the next), the precipitation variance would decrease by the trivial scaling factor L^{-2} . In superparametrization, however, the averaging will be done over the far smaller number of high-resolution grid cells, M , that one can afford to run per coarse model grid box of size $L_G \times L_G$. The variance in the uncorrelated case will then decrease by a factor of M^{-1} instead of L_G^{-2} , where L_G is measured in units of the fine resolution grid size.

This problem has the potential to be serious. If the CRM grid is 4 km, and the large-scale model grid is 200 km so that $L_G = 50$, for the uncorrelated case the variance at the 200 km scale should be a factor of $1/2500$ as large as at the 4 km scale. If only 16 CRM points are actually run in that region (assuming they continue to behave as they would in the fully resolved case), then the variance would decrease only by a factor $1/16$, resulting in a 156-fold overestimate of the variance.

The long-range correlations found in the critical region change this dramatically. Peters & Neelin (2006) found that while subcritical microwave-estimated precipitation variance below criticality scales roughly by the trivial scaling above, in the critical region precipitation variance scales as $L^{-0.46}$. With the caveat that this has only been determined within the range from $L = 25$ to 200 km, we can examine the implications of this non-trivial scaling. For the example above, variance at the 200 km scale would then be only decreased by a factor of $50^{-0.46} = 0.17$. Using the same scaling for a three-dimensional CRM with 16 points in the horizontal yields a factor of $M^{-0.46/2} = 0.53$. The overestimate is thus only by a factor of three. Similar effects should apply for a two-dimensional CRM (e.g. figure 1*b*), although the scaling probably differs.

These examples provide only a very rough illustration of the issue. Many additional factors can enter: feedbacks between the large scale and the CRM in the superparametrization may alter the statistics; numerical factors such as excess diffusivity may affect the CRM variance; and because superparametrization (and convective parametrization in general) interrupts turbulent cascades between the plume scale and large scale, more sophisticated treatment may be necessary. Nonetheless, knowledge of the empirical scaling may aid in assessing such impacts.

A converse of this quick calculation is to consider implications of the spatial scaling for the fluctuations about QE that one should aim to reproduce at different model grid sizes. Increasing L_G by a factor of 8 in the $L^{-0.46}$ scaling yields only a reduction of 0.4 in the variance near critical, and only 0.3 for a factor of 16 in L_G . Thus even on coarse model grids, variance about traditional QE remains an important effect to capture.

6. Discussion

(a) Reinterpreting QE

There are a number of important pragmatic issues regarding the implementation and consequences of convective QE, involving the boundary layer versus the free

troposphere and the temperature and moisture structure. On short time scales, variations in temperature occur about the deep tropospheric structure characteristic of QE postulates, although at larger time and space scales the free troposphere tends to match QE expectations. Variations in the vertical structure of convective heating about that predicted by QE can have substantial impacts in stochastic schemes. The importance of free tropospheric water vapour places a premium on representation of entrainment; as a by-product, it makes column water vapour—for which we have abundant observations—a good indicator of conditions conducive to convection. While important for revising convective schemes, the issues of vertical structure are less fundamental to the principle of QE than are the following considerations, which suggest a reinterpretation of QE.

A number of these features are illustrated in figure 8, which overlays a schematic of the observed features on the empirically determined critical surface for column water vapour as a function of temperature from figure 5*b*. The sharp pickup in precipitation at a particular set of values of temperature and moisture corresponds qualitatively to the original QE postulate. Interpreting precipitation as our observable for strong convection and dissipation of buoyancy and allowing for the fact that we have expressed our diagram with different temperature- and moisture-related variables, there is a qualitative correspondence to Arakawa's diagram 1*a* for the original QE postulate.

However, as argued in Peters & Neelin (2006), the empirical properties of the onset of convection correspond closely to properties of a continuous phase transition. This implies that the transition associated with QE is inseparable from a number of important statistical properties.

- The ensemble-average precipitation does not increase linearly with the distance from criticality. With a functional form like equation (4.1), there would not be a single convective time scale as in a linear relationship.
- High precipitation variance near criticality (where the system spends much of its time) is expected even in absence of changes in the large-scale forcing.
- This precipitation variance has a non-trivial scaling under spatial averaging in the critical region, corresponding to long-range (power-law) spatial correlations. The variance decreases with spatial averaging much less quickly than for independent points, so spatial averaging is not very effective at establishing the large-ensemble average envisioned in the original QE postulate. For instance, a factor of 64 increases in grid box area yields only a factor of 0.4 in variance.
- These long-range correlations are associated with scale-free critical clusters reflected in the event sizes in figure 6*b* and Peters *et al.* (2002), as well as in the broad size distributions of mesoscale convective systems (Mapes & Houze 1993; Houze 2004; Nesbitt *et al.* 2006; O. Peters *et al.* 2008, unpublished work).

The transition further exhibits dynamics characteristic of self-organized criticality as described in §§5 and 4. While the above properties are shared by all (including equilibrium) critical systems, below we present dynamical aspects specific to self-organized non-equilibrium critical systems.

- The probability density function for column water vapour exhibits a sharp drop near critical. This is associated with the sharply increasing sink for water vapour/buoyancy above criticality.

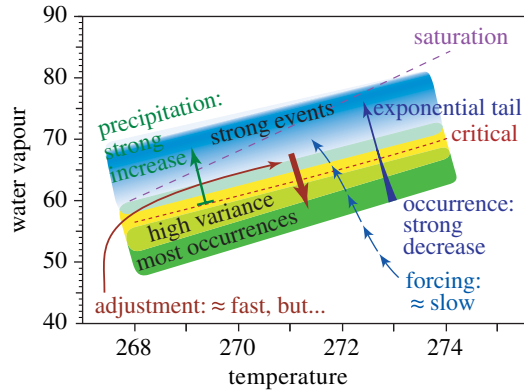


Figure 8. Schematic based on figure 5*b* illustrating the ingredients of an updated interpretation of convective QE. The critical value of column water vapour w_c at which the onset of strong convection occurs is shown as a function of vertically averaged tropospheric temperature \hat{T} . Under conventional QE, one expects the sharp increase in the expected value of precipitation above criticality and the system to spend much of its time near criticality. Additional properties are bundled with this: high precipitation variance near criticality, long-range correlations with associated clusters in precipitation near criticality and an event-size distribution with a scale-free range. While the probability of occurrence of a given (w, \hat{T}) state drops rapidly at criticality, long exponential tails of the distribution yield relatively frequent occurrence above criticality. These effects apply even when the adjustment process can be assumed to be fast.

- For precipitating points, the PDF has a peak below criticality, i.e. the system spends much of its time close to the critical point, as envisioned under QE. However, the width of the distribution is substantial. For the approximately Gaussian core, plus or minus 1 standard deviation covers the region from roughly $0.8 w_c$ to w_c , for points measured at a scale of $(25 \text{ km})^2$.
- Above criticality, the PDF for water vapour has an approximately exponential tail. Relative to a Gaussian, this slow decay above criticality implies relatively frequent occurrences of high precipitation. This behaviour is commonly observed in forced advection–diffusion processes.

The high variance near criticality is one of the clearest differences from convective QE as originally conceived. A large fraction of the precipitation occurs in the critical region, with another substantial contribution from the excursions above criticality (approx. 70 and 25%, respectively, for the observations in §4). It is thus not surprising that QE schemes have tended to be deficient in precipitation variance, with both temperature and moisture pinned too close to the postulated equilibrium. These are aspects that stochastic convective schemes and superparametrization aim to address, and both have the potential to incorporate information from the observations presented here.

(b) Conjectures for stochastic convection schemes

Given that conventional aspects of convection schemes are in need of revision to include such information as the dependence on tropospheric water vapour, and given the unfortunate sensitivity to the details of implementation in both types of parametrization, it makes sense to rethink both conventional and stochastic

aspects together. Approaches seeking to constrain the stochastic processes from observations and CRMs appear promising, along with basic principles such as care to conserve moist static energy.

The manner in which observations of precipitation, water vapour and temperature collapse to simple dependences expected from critical phenomena summarized above is highly suggestive. The fact that some of these properties occur commonly in simple systems, including lattice models as seen in the parallels between figures 6 and 7, suggests that we ought to be able to capture them in our convective schemes. The fact that some properties are universal implies that they do not provide a test of whether a system contains the correct physics for convection, but systems that aim to represent the statistics of convection should include them. It also suggests that systems simpler than fully resolving convection can be devised that will include some of these properties that have now been so clearly observed for convection.

One promising approach, adapting lattice models for use at the subgrid scale, has been initiated (Majda & Khouider 2002; Khouider *et al.* 2003). While the specifics of the moist physics based on CIN do not match the observations here, the approach is adaptable to different physics, whether from meteorology or other systems (Katsoulakis *et al.* 2003). The key points of neighbour interactions at the subgrid scale are included at low computational cost—the challenge is to accurately implement the complex physics of convection onset into a binary on/off representation at the convective scale. Empirical evaluation of transition probabilities should aid in this endeavour.

On the more computationally intensive side of the proposed solutions, these properties may be approximated in models that attempt to coarsely resolve convection (Kuang *et al.* 2005; Pauluis & Garner 2006; Knutson *et al.* 2007), and this should be investigated. Checking these properties in CRMs will also help to isolate the physics, in particular whether the plume scale is sufficient or cloud microphysics, such as aggregation and fallout processes, is involved. There is reason to believe that the network of superparametrization CRM points envisioned by Randall *et al.* (2003) should be able to capture some aspects of the long-range correlation seen in the observations, and it is posited that the long-range correlations should help with the issue of correctly estimating grid-scale variance from a small sample of points. Examination of superparametrization strategies to determine whether they can yield the same exponents as a full grid will be of interest.

Between these two approaches in terms of computational intensity, there is room for schemes similar to recent stochastic approaches, adapting convective plume models akin to those from conventional parametrizations, but including stochastic representations of the subgrid-scale fluctuations. Conjectures based on the observational results here suggest that carrying water vapour at slightly higher resolution than the wind field to interact with parametrized convective plumes might aid in capturing the exponential tail of the water vapour distribution above criticality.

An appealing conjecture for such next generation schemes comes from analogy with certain other systems exhibiting critical phenomena. Conventional parametrizations are the equivalent of mean field theory in that individual elements interact only with the large-scale mean. While mean field theory can approximate the pickup of an order parameter in a phase transition, albeit with incorrect exponent, its usefulness is often limited (e.g. Yeomans 1992) by non-negligible effects of

fluctuations. The mesoscale literature already provides a list of positive near-neighbour feedbacks (e.g. Mapes (1993), Redelsperger *et al.* (2000), Tompkins (2001), Houze (2004), Moncrieff & Liu (2006) and references therein), including: uplift by cold pools; mesoscale surface-flux enhancement; seeding from mesoscale anvils; and water vapour increases in the vicinity of previous plumes by detrainment, rain re-evaporation or baroclinic wave convergence. Inclusion of interaction among subgrid-scale plumes may thus be a key to capturing the phenomena noted here. Fortunately, the long-range correlations imply that the exact details of the physics should not be necessary to obtain the properties of §6a, opening the door to parametrizations that approximate these interactions cheaply.

This work was supported under National Science Foundation ATM-0082529 and OPP-0129800 (JWL), National Oceanic and Atmospheric Administration NA05-OAR4311134 and NA05-OAR4310007 and the Guggenheim Foundation (JDN). TMI data are from Remote Sensing Systems. We thank A. Arakawa, C. Bretherton, K. Emanuel, M. Moncrieff and D. Randall for discussions and J. Meyerson for graphical assistance.

References

- Arakawa, A. 2004 The cumulus parameterization problem: past present and future. *J. Clim.* **17**, 2493–2525. (doi:10.1175/1520-0442(2004)017<2493:RATCPP>2.0.CO;2)
- Arakawa, A. & Schubert, W. H. 1974 Interaction of a cumulus cloud ensemble with the large-scale environment Part I. *J. Atmos. Sci.* **31**, 674–701. (doi:10.1175/1520-0469(1974)031<0674:IOACCE>2.0.CO;2)
- Berner, J., Shutts, G. & Palmer, T. 2005 Parameterising the multiscale structure of organised convection using a cellular automaton. In *ECMWF Workshop on Representation of Sub-grid Processes Using Stochastic-dynamic Models, Reading, UK, June 2005*.
- Betts, A. K. & Miller, M. J. 1986 A new convective adjustment scheme. Part II: single column tests using GATE wave, BOMEX, ATEX and Arctic air-mass data sets. *Quart. J. R. Meteorol. Soc.* **112**, 693–709. (doi:10.1256/smsqj.47307)
- Bretherton, C. S., Peters, M. E. & Back, L. 2004 Relationships between water vapor path and precipitation over the tropical oceans. *J. Clim.* **17**, 1517–1528. (doi:10.1175/1520-0442(2004)017<1517:RBWVPA>2.0.CO;2)
- Brown, R. G. & Bretherton, C. S. 1997 A test of the strict quasi-equilibrium theory on long space and time scales. *J. Atmos. Sci.* **5**, 624–638. (doi:10.1175/1520-0469(1997)054<0624:ATOTSQ>2.0.CO;2)
- Brown, R. G. & Zhang, C. 1997 Variability of midtropospheric moisture and its effect on cloud-top height distribution during TOGA COARE. *J. Atmos. Sci.* **54**, 2760–2774. (doi:10.1175/1520-0469(1997)054<2760:VOMMAI>2.0.CO;2)
- Buizza, R., Miller, M. & Palmer, T. N. 1999 Stochastic representation of model uncertainties in the ECMWF ensemble prediction system. *Quart. J. R. Meteorol. Soc.* **125**, 2887–2908. (doi:10.1256/smsqj.56005)
- Ciesielski, P. E., Hartten, L. & Johnson, R. H. 1997 Impacts of merging profiler and rawinsonde winds on impacts of merging profiler and rawinsonde winds on TOGA COARE analyses. *J. Atmos. Oceanic Technol.* **14**, 1264–1279. (doi:10.1175/1520-0426(1997)014<1264:IOMPAR>2.0.CO;2)
- Cohen, B. G. & Craig, G. C. 2006 Fluctuations in an equilibrium convective ensemble. Part II: numerical experiments. *J. Atmos. Sci.* **63**, 2005–2015. (doi:10.1175/JAS3710.1)
- Craig, G. C. & Cohen, B. G. 2006 Fluctuations in an equilibrium convective ensemble. Part I: theoretical formulation. *J. Atmos. Sci.* **63**, 1996–2004. (doi:10.1175/JAS3709.1)

- Derbyshire, S. H., Beau, I., Bechtold, P., Grandpeix, J.-Y., Piriou, J.-M., Redelsperger, J.-L. & Soares, P. M. M. 2004 Sensitivity of moist convection to environmental humidity. *Quart. J. R. Meteorol. Soc.* **130**, 3055–3079. (doi:10.1256/qj.03.130)
- Dickman, R., Vespignani, A. & Zapperi, S. 1998 Self-organized criticality as an absorbing-state phase transition. *Phys. Rev. E* **57**, 5095–5105. (doi:10.1103/PhysRevE.57.5095)
- Emanuel, K. A. 1991 A scheme for representing cumulus convection in large-scale models. *J. Atmos. Sci.* **48**, 2313–2335. (doi:10.1175/1520-0469(1991)048<2313:ASFRCC>2.0.CO;2)
- Emanuel, K. A. 1993 The effect of convective response time on WISHE modes. *J. Atmos. Sci.* **50**, 1763–1775. (doi:10.1175/1520-0469(1993)050<1763:TEOCRT>2.0.CO;2)
- Emanuel, K. A. 1994 *Atmospheric convection*, p. 580. New York, NY: Oxford University Press.
- Emanuel, K. A., Neelin, J. D. & Bretherton, C. S. 1994 On large-scale circulations in convecting atmospheres. *Quart. J. R. Meteorol. Soc.* **120**, 1111–1143. (doi:10.1002/qj.49712051902)
- Eskridge, R. E., Alduchov, O. A., Chernykh, I. V., Panmao, Z., Polansky, A. C. & Doty, S. R. 1995 A comprehensive aerological reference data set (CARDS): rough and systematic errors. *Bull. Am. Meteorol. Soc.* **76**, 1759–1775. (doi:10.1175/1520-0477(1995)076<1759:ACARDS>2.0.CO;2)
- Gollub, J. P., Clarke, J., Gharib, M., Lane, B. & Mesquita, O. N. 1991 Fluctuations and transport in a stirred fluid with a mean gradient. *Phys. Rev. Lett.* **67**, 3507–3510. (doi:10.1103/PhysRevLett.67.3507)
- Grabowski, W. W. 2001 Coupling cloud processes with the large-scale dynamics using the cloud-resolving convection parameterization (CRCP). *J. Atmos. Sci.* **58**, 978–997. (doi:10.1175/1520-0469(2001)058<0978:CCPWTL>2.0.CO;2)
- Grabowski, W. W. 2003 MJO-like coherent structures: sensitivity simulations using the cloud-resolving convection parameterization (CRCP). *J. Atmos. Sci.* **60**, 847–864. (doi:10.1175/1520-0469(2003)060<0847:MLCSSS>2.0.CO;2)
- Gregory, D. & Rowntree, P. R. 1990 A mass flux convection scheme with representation of cloud ensemble characteristics and stability-dependent closure. *Mon. Wea. Rev.* **118**, 1483–1506. (doi:10.1175/1520-0493(1990)118<1483:AMFCSW>2.0.CO;2)
- Haertel, P. T. & Kiladis, G. N. 2004 Dynamics of 2-day equatorial waves. *J. Atmos. Sci.* **61**, 2707–2721. (doi:10.1175/JAS3352.1)
- Hilburn, K. A. & Wentz, F. J. 2007 Intercalibrated passive microwave rain products from the unified microwave ocean retrieval algorithm (UMORA). *J. Appl. Meteorol. Clim.* **47**, 778–794. (doi:10.1175/2007JAMC1635.1)
- Holloway, C. E. & Neelin, J. D. 2007 The convective cold top and quasi equilibrium. *J. Atmos. Sci.* **64**, 1467–1487. (doi:10.1175/JAS3907.1)
- Houze, R. A. J. 2004 Mesoscale convective systems. *Rev. Geophys.* **42**, RG4003. (doi:10.1029/2004RG000150)
- Kain, J. S. & Fritsch, J. M. 1990 A one-dimensional entraining/detraining plume model and its application in convective parameterization. *J. Atmos. Sci.* **47**, 2784–2802. (doi:10.1175/1520-0469(1990)047<2784:AODEPM>2.0.CO;2)
- Katsoulakis, M. A., Majda, A. J. & Vlachos, D. G. 2003 Coarse-grained stochastic processes for microscopic lattice systems. *Proc. Natl Acad. Sci. USA* **100**, 782–787. (doi:10.1073/pnas.242741499)
- Khairoutdinov, M. F. & Randall, D. A. 2001 A cloud resolving model as a cloud parameterization in the NCAR community climate system model: preliminary results. *Geophys. Res. Lett.* **28**, 3617–3720. (doi:10.1029/2001GL013552)
- Khouider, B., Majda, A. J. & Katsoulakis, M. A. 2003 Coarse-grained stochastic models for tropical convection and climate. *Proc. Natl Acad. Sci. USA* **100**, 11 941–11 946. (doi:10.1073/pnas1634951100)
- Knutson, T. R., Sirutis, J. J., Garner, S. T., Held, I. M. & Tuleya, R. E. 2007 Simulation of the recent multidecadal increase of atlantic hurricane activity using an 18-km-grid regional model. *Bull. Am. Meteorol. Soc.* **88**, 1549–1565. (doi:10.1175/BAMS-88-10-1549)

- Kuang, Z. & Bretherton, C. S. 2006 A mass-flux scheme view of a high-resolution simulation of a transition from shallow to deep cumulus convection. *J. Atmos. Sci.* **63**, 1895–1909. (doi:10.1175/JAS3723.1)
- Kuang, Z., Blossey, P. N. & Bretherton, C. S. 2005 A new approach for 3D cloud-resolving simulations of large-scale atmospheric circulation. *Geophys. Res. Lett.* **32**, L02809. (doi:10.1029/2004GL021024)
- Kueller, V., Gassmann, A. & Bott, A. 2007 Towards a new hybrid cumulus parameterization scheme for use in non-hydrostatic weather prediction models. *Quart. J. R. Meteorol. Soc.* **133**, 479–490. (doi:10.1002/qj.28)
- Lin, J. W.-B. & Neelin, J. D. 2000 Influence of a stochastic moist convective parameterization on tropical climate variability. *Geophys. Res. Lett.* **27**, 3691–3694. (doi:10.1029/2000GL011964)
- Lin, J. W.-B. & Neelin, J. D. 2002 Considerations for stochastic convective parameterization. *J. Atmos. Sci.* **59**, 959–975. (doi:10.1175/1520-0469(2002)059<0959:CFSCP>2.0.CO;2)
- Lin, J. W.-B. & Neelin, J. D. 2003 Toward stochastic moist convective parameterization in general circulation models. *Geophys. Res. Lett.* **30**, 1162. (doi:10.1029/2002GL016203)
- Lübeck, S. 2000 Moment analysis of the probability distribution of different sandpile models. *Phys. Rev. E* **61**, 204–209. (doi:10.1103/PhysRevE.61.204)
- Majda, A. J. 1993 The random uniform shear layer: an explicit example of turbulent diffusion with broad tail probability distributions. *Phys. Fluids A: Fluid Dyn.* **5**, 1963–1970. (doi:10.1063/1.858823)
- Majda, A. J. & Khouider, B. 2002 Stochastic and mesoscale models for tropical convection. *Proc. Natl Acad. Sci. USA* **99**, 1123–1128. (doi:10.1073/pnas.032663199)
- Maloney, E. D. & Hartmann, D. L. 2001 The sensitivity of intraseasonal variability in the NCAR CCM3 to changes in convective parameterization. *J. Clim.* **14**, 2015–2034. (doi:10.1175/1520-0442(2001)014<2015:TSOIVI>2.0.CO;2)
- Manna, S. S. 1991 Two-state model of self-organized criticality. *J. Phys. A Math. Gen.* **24**, L363–L369. (doi:10.1088/0305-4470/24/7/009)
- Mapes, B. E. 1993 Gregarious tropical convection. *J. Atmos. Sci.* **50**, 2026–2037. (doi:10.1175/1520-0469(1993)050<2026:GTC>2.0.CO;2)
- Mapes, B. E. & Houze, R. A. 1993 Cloud clusters and superclusters over the oceanic warm pool. *Mon. Weather Rev.* **121**, 1398–1415. (doi:10.1175/1520-0493(1993)121<1398:CCASOT>2.0.CO;2)
- Moncrieff, M. W. & Klinker, E. 1997 Organized convective systems in the tropical western Pacific as a process in general circulation models: a TOGA-COARE case-study. *Quart. J. R. Meteorol. Soc.* **123**, 805–827. (doi:10.1002/qj.49712354002)
- Moncrieff, M. W. & Liu, C. 2006 Representing convective organization in prediction models by a hybrid strategy. *J. Atmos. Sci.* **63**, 3404–3420. (doi:10.1175/JAS3812.1)
- Moorthi, S. & Suarez, M. J. 1992 Relaxed Arakawa–Schubert: a parameterization of moist convection for general circulation models. *Mon. Weather Rev.* **120**, 978–1002. (doi:10.1175/1520-0493(1992)120<0978:RASAPO>2.0.CO;2)
- Neelin, J. D. & Zeng, N. 2000 A quasi-equilibrium tropical circulation model—formulation. *J. Atmos. Sci.* **57**, 1741–1766. (doi:10.1175/1520-0469(2000)057<1741:AQETCM>2.0.CO;2)
- Nesbitt, S., Cifelli, W. R. & Rutledge, S. A. 2006 Storm morphology and rainfall characteristics of TRMM precipitation features. *Mon. Weather Rev.* **134**, 2702–2721. (doi:10.1175/MWR3200.1)
- Palmer, T. N. 2001 A nonlinear dynamical perspective on model error: a proposal for non-local stochastic-dynamic parameterization in weather and climate prediction models. *Quart. J. R. Meteorol. Soc.* **127**, 279–304. (doi:10.1002/qj.49712757202)
- Pan, D.-M. & Randall, D. A. 1998 A cumulus parameterization with a prognostic closure. *Quart. J. R. Meteorol. Soc.* **124**, 949–981. (doi:10.1256/smsqj.54713)
- Parsons, D. B., Yoneyama, K. & Redelsperger, J.-L. 2000 The evolution of the tropical western Pacific atmosphere–ocean system following the arrival of a dry intrusion. *Quart. J. R. Meteorol. Soc.* **126**, 517–548. (doi:10.1002/qj.49712656307)
- Pauluis, O. & Garner, S. 2006 Sensitivity of radiative-convective equilibrium simulations to horizontal resolution. *J. Atmos. Sci.* **63**, 1910–1923. (doi:10.1175/JAS3705.1)

- Peters, O. & Neelin, J. D. 2006 Critical phenomena in atmospheric precipitation. *Nat. Phys.* **2**, 393–396. (doi:10.1038/nphys314)
- Peters, H., Hertlein, C. & Christensen, K. 2002 A complexity view of rainfall. *Phys. Rev. Lett.* **88**, 018 701. (doi:10.1103/PhysRevLett.88.018701)
- Pierrehumbert, R. T. 2000 Lattice models of advection-diffusion. *Chaos Interdiscip. J. Nonlin. Sci.* **10**, 61–74. (doi:10.1063/1.166476)
- Plant, R. S. & Craig, G. C. 2008 A stochastic parameterization for deep convection based on equilibrium statistics. *J. Atmos. Sci.* **65**, 87–105. (doi:10.1175/2007JAS2263.1)
- Randall, D., Khairoutdinov, M., Arakawa, A. & Grabowski, W. 2003 Breaking the cloud parameterization deadlock. *Bull. Am. Meteor. Soc.* **84**, 1547–1564. (doi:10.1175/BAMS-84-11-1547)
- Raymond, D. J. 1997 Boundary layer quasi-equilibrium (BLQ). In *The physics and parameterization of moist atmospheric convection* (ed. R. K. Smith), pp. 387–397. Dordrecht, The Netherlands: Kluwer Academic Publishers.
- Raymond, D. J. 2000 Thermodynamic control of tropical rainfall. *Quart. J. R. Meteorol. Soc.* **126**, 889–898. (doi:10.1256/smsqj.56405)
- Redelsperger, J., Guichard, F. & Mondon, S. 2000 A parameterization of mesoscale enhancement of surface fluxes for large-scale models. *J. Clim.* **13**, 402–421. (doi:10.1175/1520-0442(2000)013<0402:APOME0>2.0.CO;2)
- Shraiman, B. I. & Siggia, E. D. 1994 Lagrangian path integrals and fluctuations in random flow. *Phys. Rev.* **49**, 2912–2927. (doi:10.1103/PhysRevE.49.2912)
- Shutts, G. J. & Palmer, T. N. 2007 Convective forcing fluctuations in a cloud-resolving model: Relevance to the stochastic parameterization problem. *J. Clim.* **20**, 187–202. (doi:10.1175/JCLI3954.1)
- Stokes, G. M. & Schwartz, S. E. 1994 The Atmospheric Radiation Measurement (ARM) program: programmatic background and design of the cloud and radiation testbed. *Bull. Am. Meteorol. Soc.* **75**, 1201–1221. (doi:10.1175/1520-0477(1994)075<1201:TARMPP>2.0.CO;2)
- Straub, K. H. & Kiladis, G. N. 2003 The observed structure of convectively coupled Kelvin waves: comparison with simple models of coupled wave instability. *J. Atmos. Sci.* **60**, 1655–1668. (doi:10.1175/1520-0469(2003)060<1655:TOSOCC>2.0.CO;2)
- Tang, C. & Bak, P. 1988 Critical exponents and scaling relations for self-organized critical phenomena. *Phys. Rev. Lett.* **60**, 2347–2350. (doi:10.1103/PhysRevLett.60.2347)
- Teixeira, J. & Reynolds, C. 2008 Stochastic nature of physical parameterizations in ensemble prediction: a stochastic convection approach. *Mon. Weather Rev.* **136**, 483–496. (doi:10.1175/2007MWR1870.1)
- Tian, B., Waliser, D., Fetzer, E., Lambriksen, B., Yung, Y. & Wang, B. 2006 Vertical moist thermodynamic structure and spatial-temporal evolution of the MJO in AIRS observations. *J. Atmos. Sci.* **63**, 2462–2485. (doi:10.1175/JAS3782.1)
- Tompkins, A. M. 2001 Organization of tropical convection in low vertical wind shears: the role of water vapor. *J. Atmos. Sci.* **58**, 529–545. (doi:10.1175/1520-0469(2001)058<0529:OOTCIL>2.0.CO;2)
- Tompkins, A. M. & Berner, J. In press. A stochastic convective approach to account for model uncertainty due to unresolved humidity variability. *J. Geophys. Res.*
- Tost, H., Jöckel, P. & Lelieveld, J. 2006 Influence of different convection parameterisations in a GCM. *Atmos. Chem. Phys.* **6**, 5475–5493.
- Uppala, S. M. *et al.* 2005 The ERA-40 re-analysis. *Quart. J. R. Meteorol. Soc.* **131**, 2961–3012. (doi:10.1256/qj.04.176)
- Xu, K.-M. & Emanuel, K. A. 1989 Is the tropical atmosphere conditionally unstable? *Mon. Weather Rev.* **117**, 1471–1479. (doi:10.1175/1520-0493(1989)117<1471:ITTACU>2.0.CO;2)
- Xu, K.-M., Arakawa, A. & Krueger, S. K. 1992 The macroscopic behavior of cumulus ensembles simulated by a cumulus ensemble model. *J. Atmos. Sci.* **49**, 2402–2420. (doi:10.1175/1520-0469(1992)049<2402:TMBOCE>2.0.CO;2)
- Yano, J.-I., Fraedrich, K. & Blender, R. 2001 Tropical convective variability as 1/f noise. *J. Clim.* **14**, 3608–3616. (doi:10.1175/1520-0442(2001)014<3608:TCVAFN>2.0.CO;2)

- Yeomans, J. 1992 *Statistical mechanics of phase transitions*. Oxford, UK: Oxford University Press.
- Yu, J.-Y. & Neelin, J. D. 1994 Modes of tropical variability under convective adjustment and the Madden–Julian oscillation. Part II: numerical results. *J. Atmos. Sci.* **51**, 1895–1914. (doi:10.1175/1520-0469(1994)051<1895:MOTVUC>2.0.CO;2)
- Zhang, G. J. & McFarlane, N. A. 1995 Sensitivity of climate simulations to the parameterization of cumulus convection in the Canadian Climate Centre general circulation model. *Atmos.-Ocean*. **33**, 407–446.
- Zhang, G. J. & Mu, M. 2005 Simulation of the Madden–Julian oscillation in the NCAR CCM₃ using a revised Zhang–McFarlane convection parameterization scheme. *J. Clim.* **18**, 4046–4064. (doi:10.1175/JCLI3508.1)
- Zhang, G. J. & Wang, H. 2006 Toward mitigating the double ITCZ problem in NCAR CCSM3. *Geophys. Res. Lett.* **33**, L06709. (doi:10.1029/2005GL025229)